Title

Empagliflozin Protects against Pulmonary Ischemia/Reperfusion Injury via an ERK1/2-Dependent Mechanism

Journal

Journal of Pharmacology and Experimental Therapeutics, 380(3)

ISSN

0022-3565

Authors

Huang, Dou
Ju, Feng
Du, Lei
et al.

Publication Date

2022-03-01

DOI

10.1124/jpet.121.000956

1521-0103/380/3/230–241$35.00
THE JOURNAL OF PHARMACOLOGY AND EXPERIMENTAL THERAPEUTICS

dx.doi.org/10.1124/jpet.121.000956
J Pharmacol Exp Ther 380:230–241, March 2022

The Journal of PHARMACOLOGY And Experimental Therapeutics

Empagliflozin Protects against Pulmonary Ischemia/Reperfusion Injury via an Extracellular Signal-Regulated Kinases 1 and 2-Dependent Mechanism

Dou Huang, Feng Ju, Lei Du, Ting Liu, Yunxia Zuo, Geoffrey W. Abbott, and Zhaoyang Hu

Department of Anesthesiology (D.H., L.D., Y.Z.) and Laboratory of Anesthesia and Critical Care Medicine, National-Local Joint Engineering Research Centre of Translational Medicine of Anesthesiology, Department of Anesthesiology (F.J., T.L., Z.H.), West China Hospital, Sichuan University, Chengdu, Sichuan, China; and Bioelectricity Laboratory, Department of Physiology and Biophysics, School of Medicine, University of California, Irvine, California, USA (G.W.A.)

Received October 7, 2021; accepted December 6, 2021

ABSTRACT

Ischemia/reperfusion (I/R) injury of the lung can lead to extensive pulmonary damage. Sodium-glucose cotransporter-2 (SGLT2) inhibitors are insulin-independent, oral antihyperglycemic agents used for treating type 2 diabetes mellitus (T2DM). Although their cardioprotective properties have been reported, their potential roles in pulmonary protection in vivo are poorly characterized. Here, we tested a hypothesis that empagliflozin, an SGLT2 inhibitor, can protect lungs in a mouse model of lung I/R injury induced by pulmonary hilum ligation in vivo. We assigned C57/BL6 mice to sham-operated, nonempagliflozin-treated control, or empagliflozin-treated groups. Pulmonary I/R injury was induced by 1-hour left hilum ligation followed by 2-hour reperfusion. Using quantitative polymerase chain reaction (q-PCR) and Western blot analysis, we demonstrate that SGLT2 is highly expressed in mouse kidney but is weakly expressed in mouse lung ($n = 5$–6 per group, $P < 0.01$ or $P < 0.001$). Empagliflozin improved respiratory function, attenuated I/R-induced lung edema, lessened structural damage, inhibited apoptosis, and reduced inflammatory cytokine production and protein concentration in bronchoalveolar lavage (BAL) fluid [$P < 0.05$ or $P < 0.001$ versus control group (CON)]. In addition, empagliflozin enhanced phosphorylation of pulmonary extracellular signal-regulated kinases 1 and 2 (ERK1/2) post-I/R injury in vivo ($P < 0.001$, versus CON, $n = 5$ per group). We further showed that pharmacological inhibition of ERK1/2 activity reversed these beneficial effects of empagliflozin. In conclusion, we showed that empagliflozin exerts strong lung protective effects against pulmonary I/R injury in vivo, at least in part via the ERK1/2-mediated signaling pathway.

SIGNIFICANCE STATEMENT

Pulmonary ischemia-reperfusion (I/R) can exacerbate lung injury. Empagliflozin is a new antidiabetic agent for type 2 diabetes mellitus. This study shows that empagliflozin attenuates lung damage after pulmonary I/R injury in vivo. This protective phenomenon was mediated at least in part via the extracellular signal-regulated kinases 1 and 2-mediated signaling pathway. This opens a new avenue of research for sodium-glucose cotransporter-2 inhibitors in the treatment of reperfusion-induced acute pulmonary injury.

Introduction

Pulmonary ischemia-reperfusion (I/R) occurs in many clinical conditions (de Perrot et al., 2003; Chen-Yoshikawa, 2021). This process is often associated with an exacerbation of lung injury, leading to heavy deterioration in lung function and altered lung histologic structure (de Perrot et al., 2003). This pulmonary I/R injury is characterized by lung edema, nonspecific alveolar damage, decreased lung compliance, and progressive hypoxemia (de Perrot et al., 2003). Therefore, strategies aimed at preventing lung I/R injury and treating specific complications may have substantial effectiveness to reduce mortality and morbidity in the postoperative period.

Empagliflozin, dapagliflozin, canagliflozin, and ertugliflozin are recently developed antidiabetic agents used in the clinical management of type 2 diabetes mellitus (T2DM). They reduce plasma glucose concentrations via regulating glucose homeostasis (Jurczak et al., 2011). In addition to their antihyperglycemic effects, in large randomized controlled trials, these sodium-glucose cotransporter-2 (SGLT2) inhibitors have exhibited the ability to improve cardiovascular outcomes and reduce heart failure hospitalizations and major adverse cardiovascular events in patients with T2DM (Zinman et al., 2015; Neal et al.,

This work was supported by the National Natural Science Foundation of China [Grant 81670300] (to Z.H.).
No author has an actual or perceived conflict of interest with the contents of this article.
dx.doi.org/10.1124/jpet.121.000956.

ABBREVIATIONS: AKT, protein kinase B; BALF, bronchoalveolar lavage fluid; CON, control; Em, empagliflozin; ERK, extracellular signal-regulated kinases; GAPDH, glyceraldehyde-3-phosphate dehydrogenase; GSK-3β, glycogen synthase kinase-3β; IL-6, interleukin-6; I/R, ischemia-reperfusion; MPO, myeloperoxidase; PCR, polymerase chain reaction; q-PCR, quantitative polymerase chain reaction; SAFE, survivor activating factor enhancement; SGLT2, sodium-glucose cotransporter 2; STAT, signal transducer and activator of transcription; T2DM, type 2 diabetes mellitus; TNF-α, tumor necrosis factor-α; TUNEL, terminal deoxynucleotidyl transferase-mediated dUTP nick-end labeling; W/D, wet-to-dry.

2017; Wiviott et al., 2019). More importantly, the most recent reports extend the substantial cardioprotective properties of SGLT2 inhibitors to nondiabetic patients (McMurray et al., 2019). Notably, accumulating evidence suggests that apart from strong cardiovascular benefits (Tentolouris et al., 2019; Sarzani et al., 2020), SGLT2 inhibitors may also protect other vital organs, for example, kidney (Ellison, 2021), liver (Yamane et al., 2019), and brain (Sa-Nguanmoo et al., 2017) in a variety of experimental animal models. In terms of the lungs, empagliflozin was shown to prevent pulmonary artery remodeling, suggesting a possible protective role of empagliflozin against vascular-related pulmonary disease (Chowdhury et al., 2020). Although empagliflozin was shown to limit infarct size after myocardial ischemia/reperfusion injury (Lu et al., 2020), the question has remained unanswered whether empagliflozin has beneficial effects against reperfusion-induced lung injury. Furthermore, it is worth exploring the underlying molecular mechanisms in potential pulmonary-protective effects with the goal of developing novel and effective therapeutic approaches to ameliorate lung damage after pulmonary I/R injury in the postoperative period.

Here, our in vivo study investigated the hypothesis that empagliflozin may attenuate lung I/R injury using a mouse model of single lung I/R injury induced by clipping the pulmonary hilum. We further elucidated an underlying molecular mechanism for this empagliflozin-induced pulmonary protection.

Materials and Methods

Animals. Animal procedures and all protocols were approved by the Institutional Animal Care and Use Committee of Sichuan University (Chengdu, Sichuan, China) (Approval No: 20211201A). This study was performed in compliance with the principles for the care and use of laboratory animals (Guide, Eighth edition, 2011). Adult, pathogen-free C57/BL6 male mice (Chengdu Dashuo Experimental Animal Co., Ltd., Chengdu, China) of average age 14 months (weighing 25 to 35 g) were used for all experiments. Mice were housed with 12:12-hour light-dark cycles at 20–25°C and fed a standard rodent diet.

Experimental Protocol. Figure 1 shows the experimental procedures. A total of 86 mice were used in the study. Specifically, 12 mice were sacrificed for the analysis of SGLT2 expression. There were another three parallel experiments to evaluate the beneficial effects of empagliflozin against lung I/R injury. Thirty-four mice were used for the determination of wet-to-dry ratio and oxygenation. Twenty-five mice were used for histologic staining, terminal deoxynucleotidyl transferase-mediated dUTP nick-end labeling (TUNEL) analysis, and Western blot analysis. Fifteen mice were used for inflammatory cytokines and myeloperoxidase measurements. Mice were allocated into five groups, as follows: (1) Sham group: Mice in the sham-operated group received once daily oral administration of physiologic saline for 7 days before thoracotomy. Lungs were exposed without ligation. n = 17. (2) Control (CON) group: Mice received physiologic saline for 7 days orally before being subjected to pulmonary I/R injury. n = 17. (3) Empagliflozin (Em) group: Empagliflozin was administered intragastrically to the mice once a day for 7 days prior to pulmonary I/R injury (10 mg/kg body weight). n = 18. (4) Control with U0126 group (CON + U0126): U0126, a mitogen-activated protein kinases (MAPK) /extracellular signal-regulated kinases (ERK) kinase specific inhibitor (1 mg/kg, MedChemExpress, Monmouth Junction, NJ), was given from the femoral vein to the control mice 5 minutes ahead of pulmonary reperfusion. n = 6. (5) Empagliflozin with U0126 group (Em + U0126): U0126 was applied to mice in the empagliflozin group. n = 6. Mice in all groups received an identical volume of vehicle. We chose the doses of empagliflozin and U0126 based on our (Hu et al., 2016; Hu et al., 2021) and others' previous publications (Oshima et al., 2019; Liu et al., 2021).

Pulmonary Ischemia and Reperfusion Injury. Animals were anesthetized with sodium pentobarbital (50 mg/kg, i.p.) and shaved over the chest. A midline neck incision was performed, and each mouse received a tracheostomy. A 20-gauge angiocatheter was introduced into the trachea, and artificial ventilation was established using a rodent MiniVent ventilator (Harvard Apparatus, Holliston, MA). The frequency was set at 110 strokes per minute, and the tidal volume was set at 0.2 ml. After stabilization, a left-side thoracotomy was performed. Left hilum was identified. Mice were injected with heparin (15 units in saline solution) 10 minutes ahead of left hilum ligation. During the lung ischemic period, the ventilator was set to a tidal volume of 0.175 ml, frequency was 120 strokes per minute. After 1 hour of pulmonary occlusion, the lung was reperfused for another 2 hours. Tidal volume was then reset at 0.2 ml; frequency was 110 strokes per minute. A heating pad was used throughout the experiment to maintain body temperature. Twenty mg/kg pentobarbital sodium (i.p.) was given every 30 minutes to each mouse to maintain anesthesia. At the end of reperfusion, 200 mg/kg (i.p.) sodium pentobarbital was used to euthanize the mice, and death was confirmed by observing the cessation of heartbeat and breath. Dissection was conducted with the aid of an operating microscope.

Arterial Blood Gas Analysis. Blood gas was measured using the ABL800 FLEX analyzer (Radiometer Medical, Brønshøj, Denmark) 120 minutes postreperfusion in the sham, control, and empagliflozin groups.

Blood Serum. Blood was obtained from the left ventricle immediately after sacrificing the mice and was centrifuged for 10 minutes (4,000 g, 4°C). The supernatant was taken and frozen at −20°C until used.

Wet-to-Dry Ratio Measurement. The left main bronchus was clamped after the mice were euthanized. The left lung lobes were taken and immediately weighed (wet weight). After that, the lung tissue was dried in an oven for 72 hours (60°C) and weighted (dry weight). The wet-to-dry (W/D) ratio was calculated and served as an index of lung water content.

Bronchoalveolar Lavage. At the end of the experiment, the right main bronchus was tied. Three aliquots of 1.5 mL phosphate-buffered saline were instilled to the left lung from the trachea. The fluid was gently aspirated after each infusion. The bronchoalveolar lavage (BAL) fluid was centrifuged at 1,500 g for 10 minutes at 4°C, and supernatant was collected and frozen for further analysis. The total protein concentration in BAL fluid was determined using a BCA Protein Assay Reagent Kit (Beyotime Institute of Biotechnology, Shanghai, China) according to manufacturers' instruction. Briefly, 1μl BAL fluid sample was mixed with 200μl BCA working reagent in a 96-well microplate and incubated in an oven for 20 minutes at 60°C. The absorbance was measured at 562 nm using a microplate reader (EPOCH, BioTek Instruments, Inc, Winooski, VT). The protein concentration is obtained based on the standard curve (Wallin et al., 2017).

Inflammatory Cytokines and Myeloperoxidase Measurements. As previously described (Zhou et al., 2019), the levels of inflammatory cytokines [interleukin-6 (IL-6) and tumor necrosis factor-α (TNF-α)] and myeloperoxidase (MPO) were measured in duplicate in BAL fluid and blood serum using enzyme-linked immunosorbent assay kits (IL-6 and MPO: MultiSciences Biotech Co., Ltd, Hangzhou, Zhejiang, China, TNF-α: Invitrogen Corp. Camarillo, CA) according to manufacturers' instructions.

Tissue Preparation. In a parallel experiment, after sacrificing the mice, the left lung was surgically dissected. The upper lobes of the lung were kept in a −80°C freezer for Western blot analysis. The lower lobes of the lung were fixed with 4% paraformaldehyde for histologic examination, immunofluorescence, and apoptosis staining.

To evaluate the expression level of SGLT2 in the lung and kidney, in a separate set of experiments, untreated C57/BL6 mice were euthanized. Then, mice lungs and kidneys were removed for quantitative

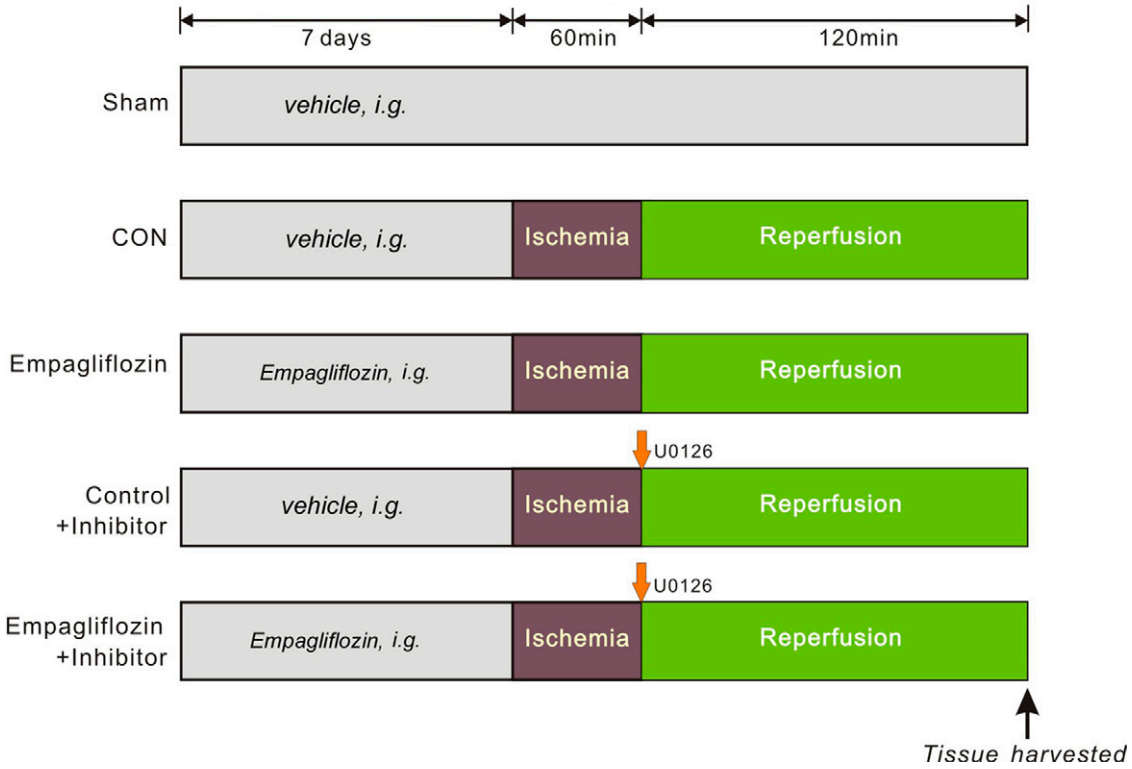

Fig. 1. Experimental protocols. Lungs in each group except for the sham-operated ones were subjected to 60 minutes of pulmonary ischemia by clamping the left hilum (ischemia), followed by 2 hours of reperfusion (reperfusion). The ERK1/2 inhibitor U0126 was given intravenously from femoral vein 5 minutes ahead of reperfusion (orange arrow). The black vertical arrow on the figure refers to the time when blood and samples were taken.

polymerase chain reaction (q-PCR), Western blot analysis, and immunofluorescence staining.

Histologic Evaluation. The lung sections were embedded in paraffin wax, and then sectioned (3 μm) for H&E staining. The histologic changes were evaluated by two independent researchers in a blinded manner. Based on the degree of neutrophil infiltration, interstitial edema, and intra-alveolar hemorrhage, a scoring system was applied for evaluation, as described previously (Matute-Bello et al., 2011; Zhou et al., 2019) (Table 1). Briefly, a score of 0 indicates normal lung histologic structure, a score of 1 indicates mild pulmonary damage, and a score of 2 indicates severe lung injury. Images were digitally captured using an upright microscope with digital camera (Eclipse Ni-E, Nikon, Tokyo, Japan).

TUNEL Assay. Cell apoptosis was determined by the TUNEL assay kit (DeadEnd Fluorometric TUNEL system, Promega Corporation, Madison, WI). A total of 10 visual fields were randomly selected and obtained from each slice. TUNEL-positive cells were stained green, and total nuclei were stained blue (DAPI). The percentage of apoptotic cells was calculated as the number of green nuclei divided by the number of blue nuclei. Images were obtained and analyzed with an upright fluorescence microscope with digital camera (Eclipse Ni-E, Nikon, Tokyo, Japan).

Quantitative Polymerase Chain Reaction Assay. We tested the mRNA expression of SGLT2 by q-PCR. TRIzol reagent (Invitrogen Life Technologies, Carlsbad, CA) was used to extract total RNA from mouse left lung and kidney. cDNA was then generated by reverse transcription. The polymerase chain reaction (PCR) system was made by the q-PCR SYBR Green mix kit (Yeasen Bio. Inc., Shanghai, China), followed by quantitative PCR on a Bio-Rad real-time PCR systems (BioRad, Hercules, CA). The housekeeper gene glyceraldehyde-3-phosphate dehydrogenase (GAPDH) was used as control. The mRNA expression levels of SGLT2 were determined via normalization to the expression of GAPDH.

The Primers:
SGLT2
Forward: 5′-GGTCTATGTTCAGAACCAAT-3′
Reverse: 5′-GAGCGCATTCCACTCAAAT-3′
GAPDH
Forward: 5′-CCACAGTCCATGCCATCACT-3′
Reverse: 5′-GATGACCTTGCCCACAGCCTT-3′

TABLE 1
Lung injury evaluation score system (Matute-Bello et al., 2011; Zhou et al., 2019)

	Score per Field		
Parameter	0	1	2
(A) Accumulation of neutrophils in the alveolar space	None	1–5	>5
(B) Accumulation of neutrophils in the interstitial space	None	1–5	>5
(C) Hyaline membrane formation	None	1	>1
(D) Presence of proteinaceous debris in the alveolar space	None	1	>1
(E) The degree of alveolar wall thickening	<2x	2x–4x	>4x
Score = [(20 × A) + (14 × B) + (7 × C) + (7 × D) + (2 × E)]/(number of fields × 100)			

The above PCR products were loaded into the wells in 2% agarose gels and then were separated by electrophoresis. Bands were visualized with UV light.

Immunofluorescence Staining. The expression of SGLT2 was also examined by immunofluorescence staining. Sections of lung and kidney were deparaffinized and rehydrated. Antigen retrieval was conducted. After being microwaved for 16 minutes and washed for 10 minutes in distilled water, the tissue slices were then blocked with 1% bovine serum albumin for 40 minutes at room temperature and incubated with SGLT2 Polyclonal Antibody (1:200; Proteintech, Wuhan Hubei China) overnight at 4°C. After blocking, the slices were washed five times with phosphate-buffered saline (5 minutes per wash) and incubated for 30 minutes with Alexa 488 goat anti-rabbit (Jackson Immunoresearch, West Grove, PA) at 37°C. DAPI (4′, 6-diamidino-2-phenylindole, Sigma-Aldrich, St. Louis, MO), a DNA-binding dye, was used for nuclear staining. Images were taken by Nikon Eclipse Ni-E fluorescence microscope (Nikon, Tokyo, Japan).

Western Blot Analysis. Tissues were washed with distilled water and then homogenized using a precooled pestle grinder (Fisher Scientific, Hampton, NH) in RIPA lysis buffer (150 mM NaCl, 1% NP-40, 50 mM Tris-HCl (pH7.4), 0.25% sodium deoxycholate, 1 mM EDTA, and 150 mM NaCl). Cocktails of phosphatase and protease inhibitor (Sigma-Aldrich, St. Louis, MO) were added in the buffer. The mixed samples were centrifuged for 10 minutes at 10,000 *g* (4°C). The supernatant was then taken. The protein concentration was determined by bicinchoninic acid (BCA) method (Pierce, Rockford, IL). The supernatant was then mixed with sample buffer (2X Laemmli, Sigma-Aldrich, St. Louis, MO), vortexed, and then boiled at 95°C for 10 minutes before loading onto 12% sodium dodecyl sulfate-PAGE gels for protein electrophoresis (12ug/well). The proteins were then transferred to nitrocellulose membranes (Pall Corporation, Port Washington, NY) and were blocked by 5% skimmed milk in 1X phosphate buffered saline solution containing 1% Tween 20 at room temperature for 45 minutes. The primary antibodies used in this study were: p-glycogen synthase kinase-3β (GSK-3β), phosphorylated GSK-3β (Ser9); t-GSK-3β, total GSK-3β; p-protein kinase B (AKT), phosphorylated AKT (ser473); t-AKT, total AKT; p-ERK, phosphorylated ERK 1/2 (Thr202/Tyr204); t-ERK, total ERK1/2; p-signal transducer and activator of transcription (STAT)-1, phosphorylated STAT-1 (Tyr701); t-STAT-1, total STAT-1; P-STAT-3, phosphorylated STAT-3 (Tyr705); t-STAT-3, total STAT-3; p-STAT-5, phosphorylated STAT-5 (Tyr694); t-STAT-5, total STAT-5 (all primary antibodies, 1:1000, Cell Signaling, Danvers, MA). SGLT2 (1:1000, Proteintech, Wuhan, Hubei, China). After overnight incubation, the membranes were incubated with goat anti-rabbit IgG secondary antibody conjugated to horseradish peroxidase (1:5000, Bio-Rad, Hercules, CA). Immunoreactive bands were visualized by the chemiluminescence ECL reagent (GE Healthcare, Little Chalfont, UK). Western blot images were taken using an Amersham Imager (600 system, GE Healthcare, Little Chalfont, UK) and were further analyzed with ImageJ (1.46r edition, National Institutes of Health, Bethesda, MD). Band densities for phosphorylated proteins were calculated relative to their respective total protein densities.

Statistical Analysis. The experimental results are shown as mean ±SD. Comparisons between groups over three were performed by one-way ANOVA followed by Newman-Keuls test or Dunnett's T3 test (if variances were not homogenous). Student's *t* tests (unpaired, two-tailed) were used to compare the means between two groups. Mann-Whitney test was used to compare the q-PCR results between two groups. Kruskal-Wallis test was applied to compare the histologic scores over three groups. A P value less than 0.05 ($P < 0.05$) was regarded as statistically significant.

Results

Expression of SGLT2 in Mice. It is well recognized that SGLT2 is dominantly located on the membrane of the renal proximal tubules (You et al., 1995). We determined the expression level of SGLT2 in mice kidneys and lungs by q-PCR, Western blot analysis, and immunofluorescence staining. Gene expression levels of SGLT2 were normalized to GAPDH. The results from q-PCR showed that SGLT2 mRNA was highly enriched in kidney biopsies obtained from mice (Fig. 2A). However, there was very little expression of SGLT2 transcript in mouse lung, i.e., approximately 0.002-fold the level we observed in the kidney (Fig. 2A). Next, the PCR products from cDNA samples were separated by electrophoresis in our study. We found that GAPDH transcript was heavily expressed in mouse

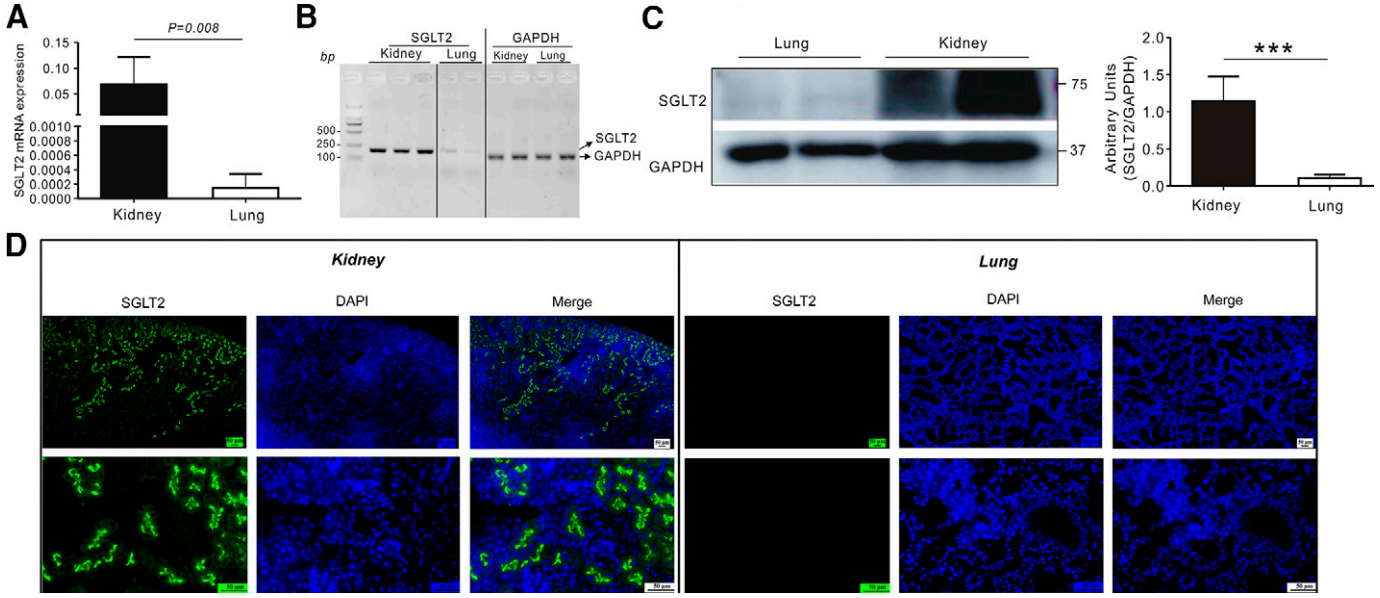

Fig. 2. SGLT2 expression. (A) Quantitative PCR validation of SGLT2 transcript expression in lungs and kidneys of mice (n = 6, each group). (B) Agarose gel electrophoresis of the PCR products obtained from A (n = 6, each group). (C) Western blot of SGLT2 protein expression in mouse lung and kidney tissue (n = 5, each group). ***$P < 0.001$, between two groups. (D) Representative images of immunofluorescence staining for SGLT2 in lung and kidney tissue sections of mice.

kidney and lung in the agarose gel (Fig. 2B). Meanwhile, mice kidney samples exhibited predominant bands around 185 bp (SGLT2) region; in contrast, the PCR product from mice lungs yielded only faint bands for SGLT2 transcript (Fig. 2B). Moreover, SGLT2 protein expression in mouse kidney or lung was also determined by Western blot method. As shown in Fig. 2C, SGLT2 was abundant in kidney, such that in mouse kidney, the SGLT2 antibody labeled a ~70-kDa protein band; however, the same band was almost absent in mouse lungs (Fig. 2C, $P < 0.01$). These findings were further confirmed by immunofluorescence staining, which demonstrated distinct staining of SGLT2 protein in the proximal tubule of the kidney, in contrast to negligible staining in the mouse lung (Fig. 2D).

Empagliflozin Attenuates Lung Damage after Pulmonary I/R Injury. Wet-to-dry (W/D) lung weight ratios (sign of lung edema) were quantified among different groups. In the present study, mice in the control group exhibited a higher W/D ratio (5.7 ±0.5) than those in the sham-operated group (4.4 ±0.4, $P < 0.001$). In contrast, the values of the W/D ratios in the empagliflozin group (4.5 ±0.2) were markedly

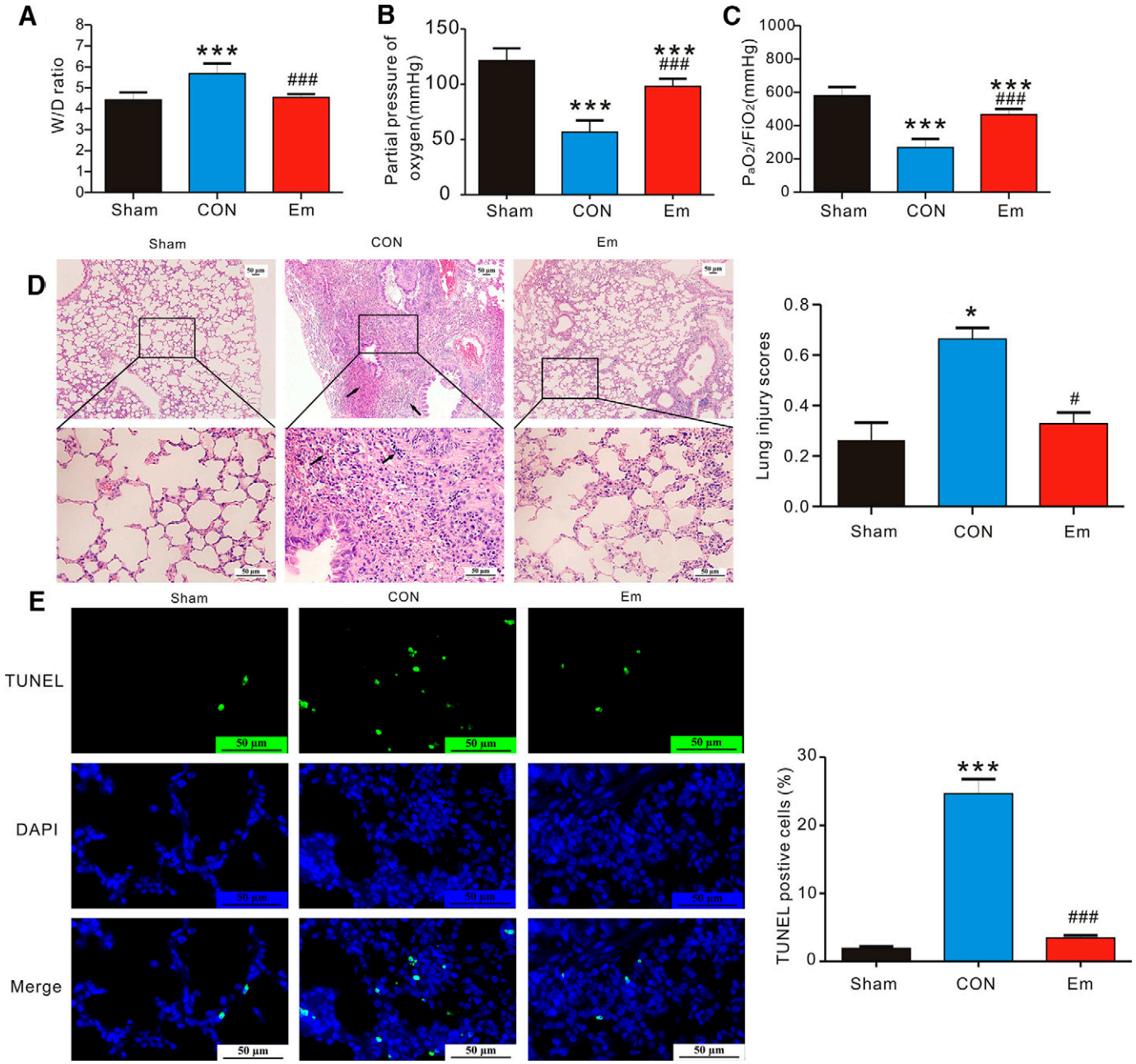

Fig. 3. Empagliflozin ameliorates pulmonary ischemia/reperfusion injury. (A) Wet-to-dry ratio of the left lung tissues post-IR. $^{***}P < 0.001$, compared with sham-operated mice; $^{\#\#\#}P < 0.001$, versus control mice. n = 6–7 per group. (B) Changes in partial pressure of oxygen post-IR. n = 6–8 per group. $^{***}P < 0.001$, versus sham-operated mice; $^{\#\#\#}P < 0.001$, versus control mice. (C) Changes in oxygenation index (PaO_2/FiO_2) post-IR. n = 6–8 per group. $^{***}P < 0.001$, compared with sham-operated mice; $^{\#\#\#}P < 0.001$, versus control mice. (D) Left: representative lung section stained for H&E after pulmonary I/R injury. Scale bars, 50μm. Representative of n = 5 mice per group. Right: semiquantitative analysis of pulmonary injury in left lungs after I/R injury (n = 5 mice per genotype). $^{***}P < 0.01$, versus sham-operated mice; $^{\#\#\#}P < 0.05$, versus control mice. (E) Left: images of TUNEL-positive cells after pulmonary I/R injury. Green, apoptotic nuclei; blue, total nuclei. Right, apoptotic index, i.e., percentage of green-stained nuclei in tissue sections. n = 5 per group. $^{***}P < 0.001$, versus sham-operated mice; $^{\#\#\#}P < 0.001$, versus control mice.

lower than those in the nonempagliflozin-treated control mice, indicating that empagliflozin could effectively reduce pulmonary edema after pulmonary IR injury (Fig. 3A). Meanwhile, we found that pO_2 and oxygenation index were decreased after reperfusion in the control group (Fig. 3, B and C, $P < 0.001$ versus sham-operated mice). However, pretreatment with empagliflozin largely improved respiratory function, as evidenced by increased pO_2 and PaO_2/FiO_2 after reperfusion injury. In accordance with improved lung function, as shown in Fig. 3D, mice in the sham and empagliflozin groups had similar histologic structures with scattered neutrophil infiltration. In contrast, acute pulmonary I/R injury led to severe alveolar damage, as indicated by extensive interstitial edema, widespread alveolar collapse and bleeding, increased alveolar interstitial thickness, and inflammatory cell infiltration. In our study, the histologic assessment of lung injury was performed using a composite histologic lung injury scoring system (see *Methods*). After reperfusion, the above-mentioned pathohistological changes were significantly alleviated in the empagliflozin-treated lungs (0.33 ±0.04) as compared with those seen in the nonempagliflozin-treated control lungs (0.66 ±0.04, $P < 0.05$). Consistent with this, although TUNEL-positive stained cells were observed in all tested groups, there were much fewer apoptotic cells in lungs with empagliflozin treatment (0.03 ±0.004), compared with those in the nonempagliflozin-treated control lungs after I/R (0.25 ±0.02, $P < 0.001$, Fig. 3E).

Empagliflozin Decreases I/R-Induced Inflammatory Cytokine Production. As shown in Fig. 4, pulmonary I/R injury caused significant elevation of IL-6 (Fig. 4, A and B) and TNF-α (Fig. 4, C and D) in BAL fluid and plasma ($P < 0.001$, compared with sham). However, levels of these proinflammatory cytokines were significantly decreased upon empagliflozin treatment ($P < 0.001$, compared with CON). MPO, a polymorphonuclear neutrophils marker enzyme, was shown to have proinflammatory properties and is associated with the pathogenesis of lung injury. The levels of MPO were also measured in our study as an index of lung inflammation. We observed that compared with sham-operated mice, pulmonary I/R injury led to a significant elevation of MPO concentration in BAL fluid (Fig. 4F) and blood serum (Fig. 4G) in control mice ($P < 0.001$ versus sham). Moreover, MPO levels were markedly reduced in the empagliflozin group than those in the control group ($P < 0.001$ versus CON, Fig. 4, F and G). Previous studies showed that high total protein concentration in BAL fluid is linked to higher mortality in patients; thus, the presence of high total protein concentration is an indicator of severe lung injury (Hendrickson et al., 2017). We also evaluated the total protein concentration in the BAL fluid post I/R. Here, as shown in Fig. 4G, we found that empagliflozin significantly inhibited the increase of total protein concentrations in bronchoalveolar lavage fluid ($P < 0.001$ versus CON), indicating that empagliflozin ameliorated acute lung damage induced by I/R injury in vivo.

Empagliflozin Affects Protein Phosphorylation after Pulmonary I/R Injury. To further elucidate potential underlying mechanisms attributable to empagliflozin-induced pulmonary protection, multiple signaling pathways associated with reperfusion injury and ischemic damage were tested in our current study. Phosphorylated proteins were normalized relative to their nonphosphorylated total proteins. We found that total GSK-3β, AKT, ERK1/2, STAT-1, STAT-3, or STAT-5 protein levels were not different in all groups. GSK-3β and AKT phosphorylation were each increased in control lungs after reperfusion injury ($P < 0.01$ or $P < 0.001$ versus sham-operated lungs), whereas phosphorylation levels of GSK-3β and AKT were expressed at almost the same levels in empagliflozin-treated or nontreated control lungs ($P > 0.05$, Fig. 5, A and B). Interestingly, although ERK phosphorylation levels in control lungs (0.6 ±0.2) were increased by 50% after 2 hours of reperfusion as compared with the sham-operated lungs (0.4 ±0.1, $P < 0.05$), we found a 2.5-fold elevation in ERK1/2 phosphorylation in

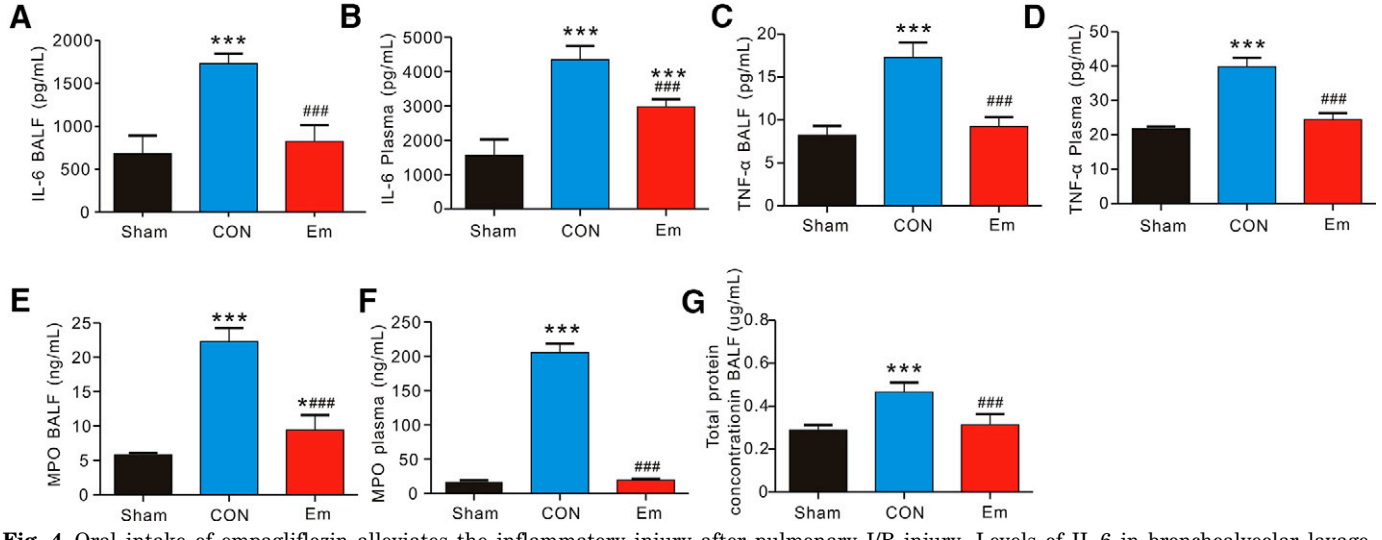

Fig. 4. Oral intake of empagliflozin alleviates the inflammatory injury after pulmonary I/R injury. Levels of IL-6 in bronchoalveolar lavage fluid (BALF) fluid (A) or in plasma (B) after 120 minutes of reperfusion. n = 4–5 per group. ***$P < 0.001$, versus sham-operated mice; $^{###}P < 0.001$, versus control mice. Levels of TNF-α in BALF fluid (C) or in plasma (D) after 120 minutes of reperfusion. n = 4–6 per group. ***$P < 0.001$, versus sham-operated mice; $^{###}P < 0.001$, versus control mice. Levels of MPO in BALF fluid (E) or in plasma (F) after 120 minutes of reperfusion. n = 4–6 per group. ***$P < 0.001$, versus sham-operated mice; $^{###}P < 0.001$, versus control mice. (G) Total protein concentration in BALF fluid after I/R injury. n = 4–5 per group. ***$P < 0.001$, versus sham-operated mice; $^{###}P < 0.001$, versus control mice.

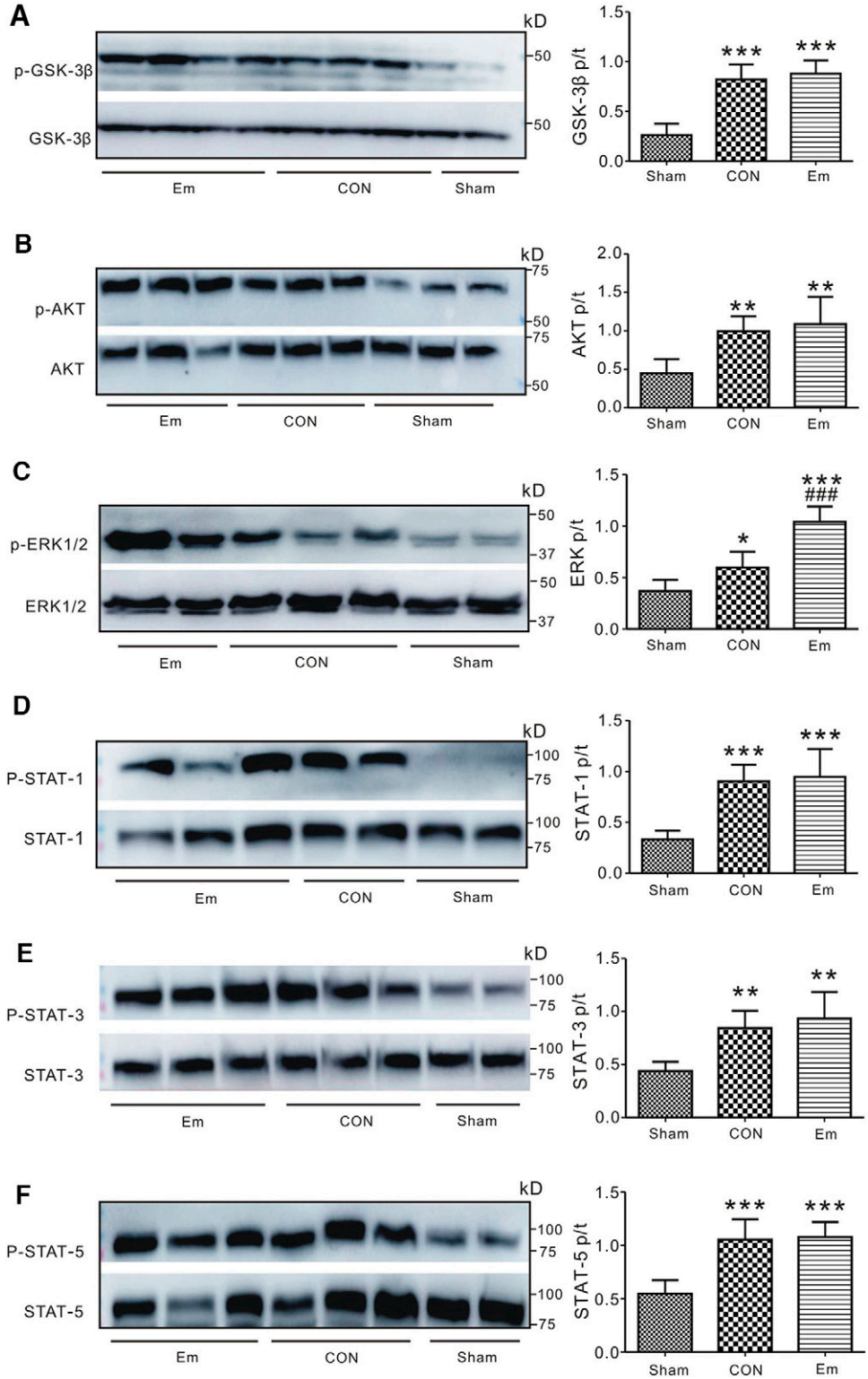

Fig. 5. The effect of empagliflozin on protein phosphorylation after I/R injury. Left: Western blots of p-GSK-3β and t-GSK-3β (A), p-AKT and t-AKT (B), p-ERK1/2 and t-ERK1/2 (C), p-STAT-1 and t-STAT-1 (D), p-STAT-3 and t-STAT-3 (E), p-STAT-5 and t-STAT-5 (F) in lung tissues after I/R injury. Right: bar graph showing mean ratio of the phospho-/total band densities. $^{**}P < 0.01$, $^{***}P < 0.001$, versus sham-operated mice; $^{\#\#\#}P < 0.001$, versus control mice. n = 5 per group.

empagliflozin-treated lungs (1.0 ±0.2) in comparison with those in control groups after I/R injury ($P < 0.001$ Fig. 5C).

STATs are a group of transcription factors with seven known members, including STAT1, STAT3, and STAT5, all of which play crucial roles in regulating cellular functions during I/R injury. As shown in Fig. 5, D–F, pulmonary reperfusion injury caused activation (phosphorylation) of STAT1 (Fig. 5D), STAT3 (Fig. 5E), and STAT5 (Fig. 5F) signaling

molecules; however, no differences were detected between CON and Em groups post I/R regardless of whether they were treated with empagliflozin (all $P > 0.05$), indicating that the beneficial pulmonary-protective effects of empagliflozin were less likely to be attributed to the modification of STAT-related pathways.

ERK1/2 Inhibition Impairs the Pulmonary-Protective Effect of Empagliflozin. We showed that the phosphorylation level of ERK1/2 was higher in control lungs than in sham-operated lungs and was further enhanced (versus CON) in the empagliflozin-treated lungs (Fig. 5C). To elucidate the potential role of ERK1/2 in empagliflozin-associated pulmonary protection, a MAPK/ERK kinase specific inhibitor, U0126, was injected to the mice in our study. Western blots indicated that U0126 administration significantly blocked empagliflozin-induced phosphorylation of ERK1/2 when compared with the non-U0126-treated empagliflozin group ($P < 0.001$, Fig. 6 A and B). We next investigated whether pharmacological inhibition of ERK1/2 activation (phosphorylation) would affect empagliflozin-induced pulmonary protection. In contrast to our earlier findings showing that empagliflozin improved lung function and reduced histologic evidence of lung damage after pulmonary I/R injury, here we found that empagliflozin-treated mice exhibited severe pulmonary damage after reperfusion in the presence of inhibitor. For example, W/D ratios were similarly elevated in U0126-treated control and U0126-treated empagliflozin groups post I/R, to levels similar to that of lungs in the non-U0126-treated control group

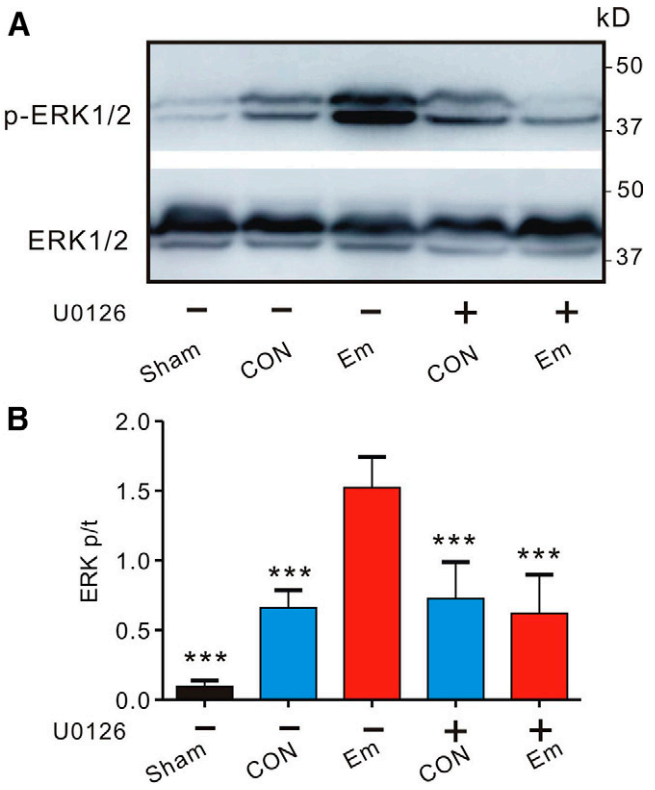

Fig. 6. U0126 abolishes empagliflozin-stimulated phosphorylation of pulmonary ERK1/2. (A) Representative Western blot of p-ERK1/2 and t-ERK1/2 in left lung tissues after I/R injury. (B) Quantification of ERK1/2 protein band density (normalized to t-ERK1/2) in mice left lungs with (+) or without (−) U0126 treatment. ***$P < 0.001$, versus empagliflozin-treated mice. n = 5 per group.

($P < 0.01$ or $P < 0.001$ versus empagliflozin group, Fig. 7A). In the meantime, U0126 pretreatment significantly diminished the PO_2 and PO_2/FiO_2 elevation we had previously seen for empagliflozin-treated mice ($P < 0.001$ versus empagliflozin group, Fig. 7, B and C). Consistent with this, empagliflozin-treated mice also treated with U0126 exhibited severe pulmonary histologic damage after I/R injury, as seen in the significantly increased lung injury scores ($P < 0.001$ versus empagliflozin group, Fig. 7, D and E). We also compared levels of pulmonary cell apoptosis between empagliflozin-treated lungs in the presence or absence of U0126. We found that U0126 induced pulmonary apoptosis, such that inhibitor-treated lungs in the empagliflozin group had more TUNEL-stained nuclei when compared with noninhibitor-treated empagliflozin lungs ($P < 0.001$ versus empagliflozin group, Fig. 7, F and G). Taken together, our results indicated that empagliflozin exerted a strong pulmonary protective effect against pulmonary I/R injury, in an ERK1/2-dependent manner.

Discussion

SGLT2 inhibitors, including empagliflozin, ertugliflozin, dapagliflozin, and canagliflozin, are oral hypoglycemic agents, initially designed for patients with T2DM (Hsia et al., 2017). SGLT2 is heavily expressed in the kidney, where it is enriched in the proximal convoluted tubule (Tentolouris et al., 2019). Accordingly, inhibition of SGLT2 results in osmotic diuresis, sodium excretion, and intravascular volume contraction (Lupsa and Inzucchi, 2018). Besides the potent antihypoglycemic properties, a large randomized EMPA-REG OUTCOME trial that recruited 7020 patients with T2DM demonstrated that empagliflozin reduced rates of death, both from cardiovascular causes and from any causes (Zinman et al., 2015). Following this, other large trials such as the DECLARE-TIMI 58 trial (Wiviott et al., 2019) and the CANVAS trial (Neal et al., 2017) all showed that other SGLT2 inhibitors, including canagliflozin and dapagliflozin, offered beneficial cardioprotective effects in patients with T2DM. Surprisingly, the follow-up analyses of the EMPA-REG OUTCOME trial (Inzucchi et al., 2018), recent DAPA-HF trial (McMurray et al., 2019), and EMPEROR-PRESERVED trial (Anker et al., 2021) all revealed that SGLT2 inhibitors exhibited cardioprotective properties regardless of the absence or presence of type 2 diabetes mellitus. In line with clinical case findings, the protective effects of SGLT2 inhibitors were also extended and confirmed in organs other than the heart (Verma and McMurray, 2018) in preclinical studies using various animal models. Focusing on acute I/R injury, recent emerging reports showed that empagliflozin could protect nondiabetic hearts against myocardial I/R injury-induced lethal arrhythmia (Hu et al., 2021). Additionally, empagliflozin (Lu et al., 2020) and dapagliflozin (Lahnwong et al., 2020) each had infarct-sparing effects after myocardial I/R injury in animals without T2DM. Unfortunately, the current knowledge about SGLT2 inhibitors in perioperative lung protection is indirect. For example, reports showed that empagliflozin had beneficial effects on bleomycin-induced pulmonary fibrosis (Kabel et al., 2020), obesity-induced asthma (Park et al., 2019), or pulmonary artery remodeling (Chowdhury et al., 2020). Therefore, our current study may shed light on the potential protective role of SGLT2 inhibitors against pulmonary I/R injury in vivo. We showed in our study that empagliflozin, a SGLT2

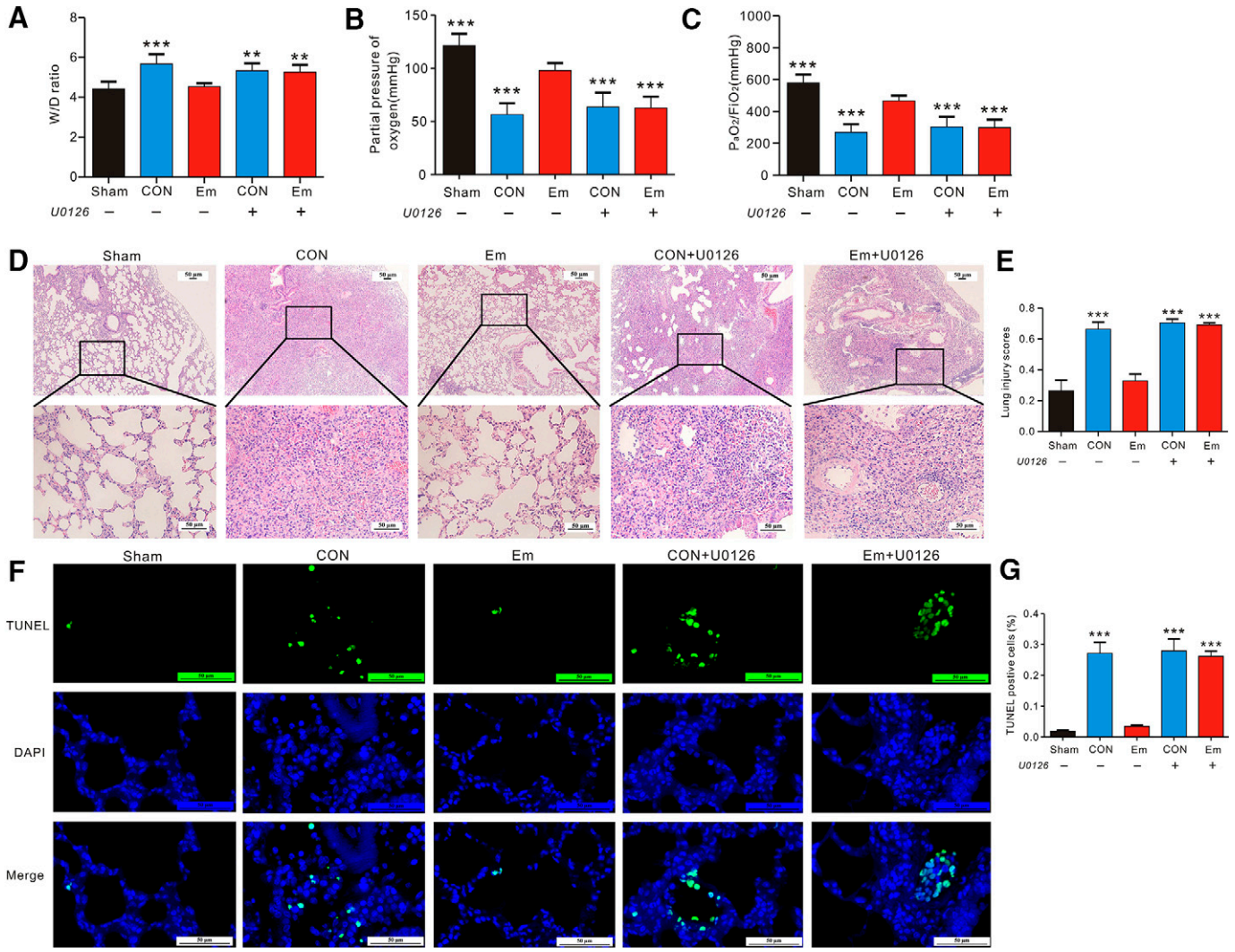

Fig. 7. Pharmacological inhibition of ERK1/2 reverses the pulmonary protection offered by empagliflozin after I/R injury. (A) Wet-to-dry ratio of left lungs from sham-operated, CON, and empagliflozin-treated mice in the absence (−) or presence (+) of U0126 after reperfusion . $^{**}P < 0.01$, $^{***}P < 0.001$, versus empagliflozin-treated mice. n = 5–7 per group. Values for sham, CON, and Em groups are repeated from Fig. 3A for comparison. (B) Changes in partial pressure of oxygen. $^{***}P < 0.001$, versus empagliflozin-treated mice. n = 6–8 per group. Values for sham, CON, and Em groups are repeated from Fig. 3B for comparison. (C) Changes in oxygenation index. $^{***}P < 0.001$, versus empagliflozin-treated mice. n = 6–8 per group. Values for sham, CON, and Em groups are repeated from Fig. 3C for comparison. (D) Representative H&E-stained left lung sections in five experimental groups. (E) Histologic evaluation of pulmonary damage after I/R injury. $^{*}P < 0.05$, $^{**}P < 0.01$, versus empagliflozin-treated mice. n = 4–5 per group. Values for sham, CON, and Em groups are repeated from Fig. 3D for comparison. (F) Representative images of TUNEL-positive cells after pulmonary I/R injury. (G) Analysis of pulmonary cell apoptosis in sham, CON, and empagliflozin-treated mice with (+) or without (−) U0126. n = 4–5 per group. $^{***}P < 0.001$, versus empagliflozin-treated mice. Values for sham, CON, and Em groups are repeated from Fig. 3E for comparison.

inhibitor, attenuated lung damage after pulmonary I/R injury. For example, it effectively reduced pulmonary edema, improved oxygenation, inhibited apoptosis, alleviated structural abnormalities, and decreased inflammatory cytokine production after pulmonary IR injury. Our results may offer new perspectives for designing individualized therapeutic strategies for patients with high risk of pulmonary injury during the perioperative period.

It has been shown that SGLT2 is primarily detected in the kidney (Kanai et al., 1994). Several investigations further showed that SGLT2 is also expressed in other tissues, like hearts and pancreatic islets in animals or humans (Sabatino et al., 2020; Saponaro et al., 2020). Unlike SGLT1, which can be found in various organs and tissues, SGLT2 is not expressed in normal human lungs according to the National Center for Biotechnology Information (NCBI) Gene database (https://www.ncbi.nlm.nih.ov/gene/6524), whereas in recent published work, Sabatino et al. reported that SGLT2 was slightly expressed in mouse lung but substantially expressed in kidney (Sabatino et al., 2020). In line with the earlier investigation, using different methodologies including q-PCR, gel electrophoresis, and Western blot analysis, we were able to detect faint SGLT2 transcript and protein expression in C57BL/6 mice lungs as shown in Fig. 2, A–C. It is worth mentioning that in our study, SGLT2 was localized and abundantly expressed in kidney proximal tubules; in contrast, no obvious positive-stained SGLT2 signals were visualized in lung sections (Fig. 2D). Meanwhile, although the antibody could detect SGLT2

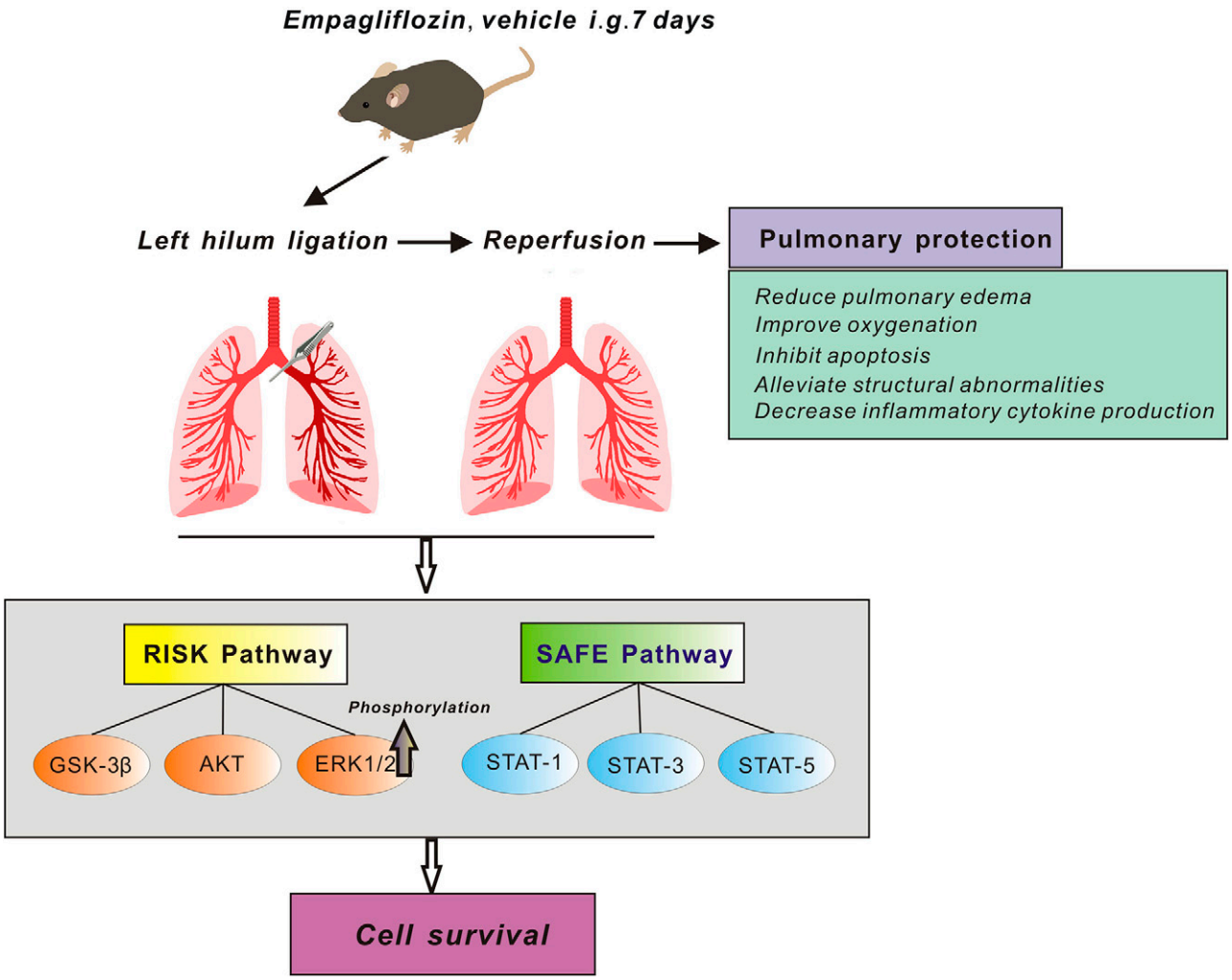

Fig. 8. Schematic illustration of the potential mechanisms of empagliflozin on pulmonary injury induced by ischemia and reperfusion.

expression in Western blotting, it failed to detect its epitopes in immunofluorescence-stained samples under a fluorescence microscope in our study (Fig. 2D). The reason may be attributed to the difference between these two techniques. Although immunofluorescence and Western blotting all rely on the antibody-antigen interaction, their detective sensitivity is different; therefore, it is rational that faint signals were unable to be visualized. Taking into account the four different methodologies we used, one can conclude that SGLT2 is weakly expressed in mouse lung (Fig. 2, A–D). Thus, our results further indicate that empagliflozin-induced lung protection in the current animal model may be exerted via an alternative mechanism rather than direct targeting of pulmonary SGLT2 receptors.

This study is the first to elucidate the beneficial role of SGLT2 inhibitors in pulmonary I/R injury, albeit they are known to alleviate I/R damage in other organs, and we further identified the underlying mechanisms involving signaling pathways (Figure 8). There are two similar but independent prosurvival signaling pathways associated with I/R injury, the reperfusion injury salvage kinase pathway and the survivor activating factor enhancement (SAFE) pathway. ERK1/2 and AKT, major components of the reperfusion injury salvage kinase pathway, can each be phosphorylated upon activation by stress such as I/R injury (Hausenloy and Yellon, 2007). It is well-established that protective stimuli, such as ischemic preconditioning and postconditioning, can cause AKT and ERK1/2 activation; thus, inhibition of their phosphorylation may abolish their beneficial protective effects (Hausenloy et al., 2011; Hu et al., 2016).

Meanwhile, GSK-3β, a downstream signaling molecule of AKT and ERK1/2 pathways, may serve as a possible point of convergence for prosurvival signals conveyed by various pathways. Our study demonstrated that empagliflozin, an SGLT2 inhibitor, exerts favorable effects in ameliorating pulmonary damage post-I/R by enhancing pulmonary phosphorylation of ERK1/2, but not AKT or GSK-3β. Furthermore, we also found that the beneficial effects were blocked by the ERK1/2 inhibitor, U0126, indicating that empagliflozin-induced pulmonary protection was exerted via an ERK1/2 phosphorylation-dependent mechanism (Fig. 7, A–G). Meanwhile, we also examined the importance of the SAFE pathway in our study. Signaling molecules including STAT-1$\sim$STAT-5 in this prosurvival cascade can be activated and phosphorylated, lessening cell death during reperfusion (Lecour, 2009). We and others have

previously found that phosphorylation of STATs was required for organ protection (Stephanou, 2004; Luo et al., 2018). However, in the current study, although we found I/R stimuli was able to stimulate STAT1, STAT3, and STAT5 activation, i.e., phosphorylation, the administration of empagliflozin failed to further enhance their phosphorylation levels, suggesting that the empagliflozin-induced pulmonary protection is unlikely to be due to the activation of SAFE pathway.

There are several limitations in this study. First, the usual dose for empagliflozin is 10mg–25mg/60kg/d for humans, whereas we used 10mg/kg/d for mice, which is beyond the currently used clinical dose range. The dose of empagliflozin we used was based on recently published articles (Oshima et al., 2019; Hu et al., 2021; Liu et al., 2021). Although we showed that empagliflozin protected lungs against pulmonary I/R injury, its lung protective properties within the typical, currently used clinical range deserve further determination. Regardless, the present study provides preliminary evidence for the potential therapeutic properties of empagliflozin against I/R-induced lung damage. Second, mice in the current study experienced 2 hours of reperfusion, which may cause acute pulmonary damage. Lung I/R injury serves as a major complication after cardiopulmonary bypass or lung transplantation; therefore, the validation of empagliflozin-induced long-term lung protection may be carried out in different animal models in the future. Third, we only evaluated two major signaling pathways associated with reperfusion injury; whether other molecules or kinases play a role in this beneficial process remains to be elucidated. Fourth, we did not use additional drugs as controls, such as tissue plasminogen activator; it would be interesting to see its effect in future studies. Fifth, we conducted three parallel experiments to evaluate the effect of empagliflozin on lung I/R injury. We found that empagliflozin attenuated lung damage after pulmonary I/R injury. However, the animal numbers are not always consistent in each set of the experiment. We therefore cannot exclude the possibility that this number difference may eventually produce bias.

In conclusion, the present results showed that pretreatment with empagliflozin exerted strong pulmonary protective effects against reperfusion-induced lung injury in vivo, which was associated with phosphorylation of pulmonary ERK1/2. Furthermore, inhibition of ERK1/2 activation abolished the empagliflozin-induced pulmonary protection. The empagliflozin-mediated pulmonary protection we observed is therefore linked to ERK1/2-dependent pathways. Given their significant protection efficacies and unique insulin-independent mode of action, SGLT2 inhibitors may offer a promising and novel therapeutic approach for patients with high risk of pulmonary damage during the perioperative period.

Authorship Contributions

Participated in research design: Hu.

Conducted experiments: Huang, Ju, Liu, Hu.

Performed data analysis: Huang, Ju, Du, Liu, Hu.

Wrote or contributed to the writing of the manuscript: Hu, Zuo, Abbott.

Acknowledgments

We would like to thank Dr. Qingjie Xia and Dr. Dunshui Liao for technical support in q-PCR.

References

Anker SD, Butler J, Filippatos G, Ferreira JP, Bocchi E, Böhm M, Brunner-La Rocca H–P, Choi D-J, Chopra V, Chuquiure-Valenzuela E, et al.; EMPEROR-Preserved Trial Investigators (2021) Empagliflozin in heart failure with a preserved ejection fraction. *N Engl J Med* **385**:1451–1461.

Chen-Yoshikawa TF (2021) Ischemia-reperfusion injury in lung transplantation. *Cells* **10**:1333.

Chowdhury B, Luu AZ, Luu VZ, Kabir MG, Pan Y, Teoh H, Quan A, Sabongui S, Al-Omran M, Bhatt DL, et al. (2020) The SGLT2 inhibitor empagliflozin reduces mortality and prevents progression in experimental pulmonary hypertension. *Biochem Biophys Res Commun* **524**:50–56.

de Perrot M, Liu M, Waddell TK, and Keshavjee S (2003) Ischemia-reperfusion-induced lung injury. *Am J Respir Crit Care Med* **167**:490–511.

Ellison DH (2021) SGLT2 inhibitors, hemodynamics, and kidney protection. *Am J Physiol Renal Physiol* **321**:F47–F49.

Hausenloy DJ, Lecour S, and Yellon DM (2011) Reperfusion injury salvage kinase and survivor activating factor enhancement prosurvival signaling pathways in ischemic postconditioning: two sides of the same coin. *Antioxid Redox Signal* **14**:893–907.

Hausenloy DJ and Yellon DM (2007) Reperfusion injury salvage kinase signalling: taking a RISK for cardioprotection. *Heart Fail Rev* **12**:217–234.

Hendrickson CM, Abbott J, Zhuo H, Liu KD, Calfee CS, and Matthay MA; NHLBI ARDS Network (2017) Higher mini-BAL total protein concentration in early ARDS predicts faster resolution of lung injury measured by more ventilator-free days. *Am J Physiol Lung Cell Mol Physiol* **312**:L579–L585.

Hsia DS, Grove O, and Cefalu WT (2017) An update on sodium-glucose co-transporter-2 inhibitors for the treatment of diabetes mellitus. *Curr Opin Endocrinol Diabetes Obes* **24**:73–79.

Hu Z, Hu S, Yang S, Chen M, Zhang P, Liu J, and Abbott GW (2016) Remote liver ischemic preconditioning protects against sudden cardiac death via an ERK/GSK-3β-dependent mechanism. *PLoS One* **11**:e0165123.

Hu Z, Ju F, Du L, and Abbott GW (2021) Empagliflozin protects the heart against ischemia/reperfusion-induced sudden cardiac death. *Cardiovasc Diabetol* **20**:199.

Inzucchi SE, Kosiborod M, Fitchett D, Wanner C, Hehnke U, Kaspers S, George JT, and Zinman B (2018) Improvement in cardiovascular outcomes with empagliflozin is independent of glycemic control. *Circulation* **138**:1904–1907.

Jurczak MJ, Lee HY, Birkenfeld AL, Jornayvaz FR, Frederick DW, Pongratz RL, Zhao X, Moeckel GW, Samuel VT, Whaley JM, et al. (2011) SGLT2 deletion improves glucose homeostasis and preserves pancreatic beta-cell function. *Diabetes* **60**:890–898.

Kabel AM, Estfanous RS, and Alrobaian MM (2020) Targeting oxidative stress, proinflammatory cytokines, apoptosis and toll like receptor 4 by empagliflozin to ameliorate bleomycin-induced lung fibrosis. *Respir Physiol Neurobiol* **273**:103316.

Kanai Y, Lee WS, You G, Brown D, and Hediger MA (1994) The human kidney low affinity Na+/glucose cotransporter SGLT2. Delineation of the major renal reabsorptive mechanism for D-glucose. *J Clin Invest* **93**:397–404.

Lahnwong S, Palee S, Apaijai N, Sriwichaiin S, Kerdphoo S, Jaiwongkam T, Chattipakorn SC, and Chattipakorn N (2020) Acute dapagliflozin administration exerts cardioprotective effects in rats with cardiac ischemia/reperfusion injury. *Cardiovasc Diabetol* **19**:91.

Lecour S (2009) Activation of the protective survivor activating factor enhancement (SAFE) pathway against reperfusion injury: does it go beyond the RISK pathway? *J Mol Cell Cardiol* **47**:32–40.

Liu Y, Wu M, Xu B, and Kang L (2021) Empagliflozin alleviates atherosclerosis progression by inhibiting inflammation and sympathetic activity in a normoglycemic mouse model. *J Inflamm Res* **14**:2277–2287.

Lu Q, Liu J, Li X, Sun X, Zhang J, Ren D, Tong N, and Li J (2020) Empagliflozin attenuates ischemia and reperfusion injury through LKB1/AMPK signaling pathway. *Mol Cell Endocrinol* **501**:110642.

Luo N, Liu J, Chen Y, Li H, Hu Z, and Abbott GW (2018) Remote ischemic preconditioning STAT3-dependently ameliorates pulmonary ischemia/reperfusion injury. *PLoS One* **13**:e0196186.

Lupsa BC and Inzucchi SE (2018) Use of SGLT2 inhibitors in type 2 diabetes: weighing the risks and benefits. *Diabetologia* **61**:2118–2125.

Matute-Bello G, Downey G, Moore BB, Groshong SD, Matthay MA, Slutsky AS, and Kuebler WM; Acute Lung Injury in Animals Study Group (2011) An official American Thoracic Society workshop report: features and measurements of experimental acute lung injury in animals. *Am J Respir Cell Mol Biol* **44**:725–738.

McMurray JJV, Solomon SD, Inzucchi SE, Køber L, Kosiborod MN, Martinez FA, Ponikowski P, Sabatine MS, Anand IS, Bělohlávek J, et al.; DAPA-HF Trial Committees and Investigators (2019) Dapagliflozin in patients with heart failure and reduced ejection fraction. *N Engl J Med* **381**:1995–2008.

Neal B, Perkovic V, Mahaffey KW, de Zeeuw D, Fulcher G, Erondu N, Shaw W, Law G, Desai M, and Matthews DR; CANVAS Program Collaborative Group (2017) Canagliflozin and cardiovascular and renal events in type 2 diabetes. *N Engl J Med* **377**:644–657.

Oshima H, Miki T, Kuno A, Mizuno M, Sato T, Tanno M, Yano T, Nakata K, Kimura Y, Abe K, et al. (2019) Empagliflozin, an SGLT2 inhibitor, reduced the mortality rate after acute myocardial infarction with modification of cardiac metabolomes and antioxidants in diabetic rats. *J Pharmacol Exp Ther* **368**:524–534.

Park HJ, Han H, Oh EY, Kim SR, Park KH, Lee JH, and Park JW (2019) Empagliflozin and dulaglutide are effective against obesity-induced airway hyperresponsiveness and fibrosis in a murine model. *Sci Rep* **9**:15601.

Sabatino J, De Rosa S, Tammè L, Iaconetti C, Sorrentino S, Polimeni A, Mignogna C, Amorosi A, Spaccarotella C, Yasuda M, et al. (2020) Empagliflozin prevents doxorubicin-induced myocardial dysfunction. *Cardiovasc Diabetol* **19**:66.

Sa-Nguanmoo P, Tanajak P, Kerdphoo S, Jaiwongkam T, Pratchayasakul W, Chattipakorn N, and Chattipakorn SC (2017) SGLT2-inhibitor and DPP-4 inhibitor improve brain function via attenuating mitochondrial dysfunction, insulin

resistance, inflammation, and apoptosis in HFD-induced obese rats. *Toxicol Appl Pharmacol* **333**:43–50.
Saponaro C, Mühlemann M, Acosta-Montalvo A, Piron A, Gmyr V, Delalleau N, Moerman E, Thévenet J, Pasquetti G, Coddeville A, et al. (2020) Interindividual heterogeneity of SGLT2 expression and function in human pancreatic islets. *Diabetes* **69**:902–914.
Sarzani R, Giulietti F, Di Pentima C, and Spannella F (2020) Sodium-glucose cotransporter-2 inhibitors: peculiar "hybrid" diuretics that protect from target organ damage and cardiovascular events. *Nutr Metab Cardiovasc Dis* **30**:1622–1632.
Stephanou A (2004) Role of STAT-1 and STAT-3 in ischaemia/reperfusion injury. *J Cell Mol Med* **8**:519–525.
Tentolouris A, Vlachakis P, Tzeravini E, Eleftheriadou I, and Tentolouris N (2019) SGLT2 inhibitors: a review of their antidiabetic and cardioprotective effects. *Int J Environ Res Public Health* **16**:2965.
Verma S and McMurray JJV (2018) SGLT2 inhibitors and mechanisms of cardiovascular benefit: a state-of-the-art review. *Diabetologia* **61**:2108–2117.
Wallin H, Kyjovska ZO, Poulsen SS, Jacobsen NR, Saber AT, Bengtson S, Jackson P, and Vogel U (2017) Surface modification does not influence the genotoxic and inflammatory effects of TiO2 nanoparticles after pulmonary exposure by instillation in mice. *Mutagenesis* **32**:47–57.
Wiviott SD, Raz I, Bonaca MP, Mosenzon O, Kato ET, Cahn A, Silverman MG, Zelniker TA, Kuder JF, Murphy SA, et al.; DECLARE–TIMI 58 Investigators (2019) Dapagliflozin and cardiovascular outcomes in type 2 diabetes. *N Engl J Med* **380**:347–357.
Yamane M, Matono T, Okano JI, Nagahara R, Matsuki Y, Okamoto T, Miyoshi KI, Sugihara T, Nagahara T, Koda M, et al. (2019) Protective effects of ipragliflozin, a sodium-glucose cotransporter 2 inhibitor, on a non-alcoholic steatohepatitis mouse model. *Yonago Acta Med* **62**:30–35.
You G, Lee WS, Barros EJ, Kanai Y, Huo TL, Khawaja S, Wells RG, Nigam SK, and Hediger MA (1995) Molecular characteristics of Na(+)-coupled glucose transporters in adult and embryonic rat kidney. *J Biol Chem* **270**:29365–29371.
Zhou L, Köhncke C, Hu Z, Roepke TK, and Abbott GW (2019) The KCNE2 potassium channel β subunit is required for normal lung function and resilience to ischemia and reperfusion injury. *FASEB J* **33**:9762–9774.
Zinman B, Wanner C, Lachin JM, Fitchett D, Bluhmki E, Hantel S, Mattheus M, Devins T, Johansen OE, Woerle HJ, et al.; EMPA-REG OUTCOME Investigators (2015) Empagliflozin, cardiovascular outcomes, and mortality in type 2 diabetes. *N Engl J Med* **373**:2117–2128.

Address correspondence to: Dr. Zhaoyang Hu, No.37 Guoxue Xiang, Wuhou District, Chengdu, Sichuan, 610041, China. E-mail: zyhu@hotmail.com